

Broadband Transparent Absorber Based on Indium Tin Oxide-Polyethylene Terephthalate Film

LIN ZHANG, YAN SHI¹, (Senior Member, IEEE), JIN XI YANG, XUAN ZHANG,
AND LONG LI¹, (Senior Member, IEEE)

School of Electronic Engineering, Xidian University, Xi'an 710071, China

Corresponding author: Yan Shi (shiyang@mail.xidian.edu.cn)

This work was supported in part by the Natural National Science Foundation of China under Grant 61771359, and in part by the Natural Science Basic Research Plan in Shaanxi Province under Grant 2018JM6006.

ABSTRACT In this paper, a broadband transparent microwave absorber with a fractional bandwidth of 118.1% was designed. In the proposed absorber, a gear-shaped unit cell consisting of optically transparent indium tin oxide-polyethylene terephthalate films fabricated on a polymethyl methacrylate is developed to guarantee electromagnetic wave to well enter into and is dissipated in the absorbing structure. Two resonant frequencies at 4.8 GHz and 13.6 GHz, which correspond to electromagnetic and electric resonances, respectively, are generated to achieve a wide absorbing band from 3.86 GHz to 15.04 GHz covering S, C, X and Ku bands. The proposed absorber has the advantages of low profile, polarization insensitivity, and angular stability. The prototype of the absorber has been fabricated and measured, and the experimental results are in good agreement with the simulation results.

INDEX TERMS Broadband, transparent, indium tin oxide-polyethylene terephthalate films, low profile, polarization insensitivity, angular stability.

I. INTRODUCTION

With rapid progress of metamaterials, absorbers based on metamaterials have been a hot topic among scientific researchers and applied into many engineering fields including electromagnetic interference and radar stealth [1], [2]. Traditional metamaterial-based absorbers [3]–[13] usually use the opaque metallic-dielectric structure, which limits greatly their applications in some special scenarios such as airplane windscreen, zenith, vehicle glasses, etc.

In recent years, a number of transparent absorbers were theoretically designed and experimentally fabricated [15]–[27]. For the optically transparent absorbers, the topology and substrate are all made of transparent materials. Among transparent absorbing designs, indium tin oxide (ITO) becomes the most widely used transparent conducting materials due to its high electrical conductivity and high transmittance in the visible and near-IR range. The ITO-based absorbers are generally composed of the patterned

ITO topology fabricated on a thin polyethylene terephthalate (PET) film [20], [22] or soda-lime glass [23]–[25]. The ITO sheets with different square resistances can act as top topology and backboard, respectively. The ITO film with small square resistance works like metal ground in the typical design, which could ensure transmitted energy as less as possible. In multilayer designs, the top and bottom PET-ITO films are separated by air spacer [20], [21] or polymethyl methacrylate (PMMA) substrate [22].

Besides optically transparent property, the transparent absorbers should have excellent performance including wide absorbing bandwidth, thin thickness, polarization insensitivity, and incident angle stability. Similar to the metamaterial-based absorbers, the perfect absorption can be achieved by specially designed topology and optimized dimensions of the transparent absorbers [27]–[29]. In order to widen absorbing band, a multi-layered structure with different patterns and corresponding sizes was proposed to obtain an absorbing band covering 8.1~28.7 GHz for the absorption of 90% [24]. However, the use of the multi-layer structure results in a high overall profile of $0.61\lambda_0$ (λ_0 is wavelength in free space

The associate editor coordinating the review of this manuscript and approving it for publication was Muhammad Zubair¹.

TABLE 1. Parameters of the transparent absorber.

Parameter	Value	Parameter	Value
p	12.9 mm	Re1	40 Ω /sq
l	3.4 mm	Re2	6 Ω /sq
r	6.2 mm	t_d	4.5 mm
g	1.1 mm	tp_1	0.175 mm
h_1	0.8 mm	tp_2	0.125 mm
h_2	0.8 mm		

at center frequency). In addition to the laminated structure, composite substrate consisting of the distilled water and PMMA substrate with an electrical thickness of $0.55\lambda_0$ was developed to achieve an over 90% absorption in a wide band from 6.4 GHz to 23.7 GHz [26]. Besides, in [27] a stereo structure was designed to obtain an absorption of better than 85% covering a frequency band of 5.5-19.7 GHz and 22.5-27.5 GHz. Unfortunately, the 3-D structure gives rise to a high profile of $0.91\lambda_0$.

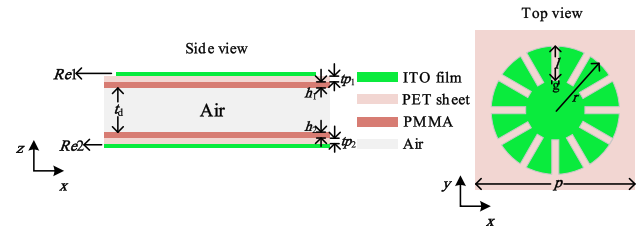
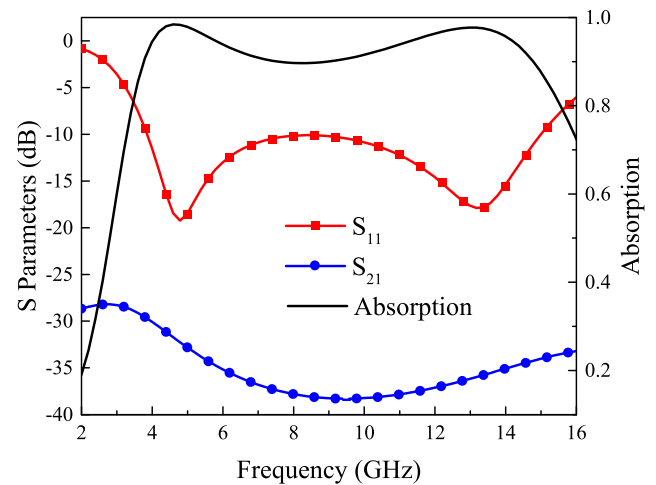
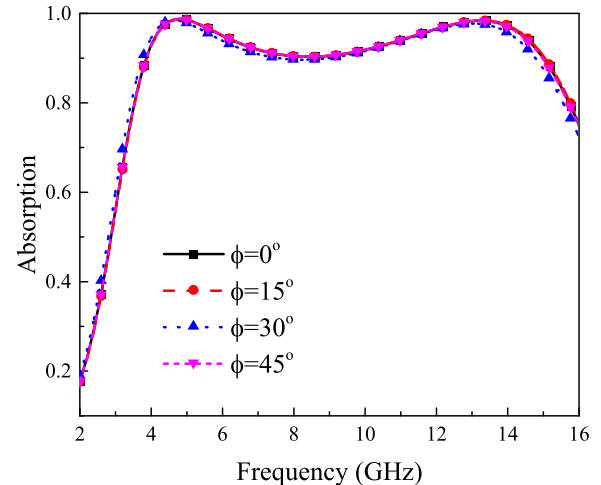
In this paper, a thin and broadband transparent absorber with a fractional bandwidth of 118.1% has been designed. A gear-shaped ITO-PET unit cell fabricated on the PMMA substrate is designed as the upper topology, and the PMMA-PET-ITO structure is used as the backboard. With the designed unit cell, two different resonant modes are simultaneously excited at 4.8 GHz and 13.6 GHz, and thus a wide absorption over 90% is achieved in a wide frequency band from 3.86 GHz to 15.04 GHz. The proposed transparent absorber has a low profile of $0.218\lambda_g$ (λ_g is the wavelength in substrate at the center frequency), polarization-insensitive property and wide incident angle characteristic due to the symmetric structure.

II. TRANSPARENT ABSORBING STRUCTURE DESIGN

A. ABSORBING STRUCTURE DESIGN

As shown in Fig. 1, the proposed absorbing unit cell is a two-layer structure with an air spacer. Each layer is a sandwich structure consisting of ITO film, PET sheet, and PMMA substrate. On the top layer, a gear-shaped ITO film is designed, while on the bottom layer a square ITO film is used. The dimensions of the unit cell are given in Table 1. The relative permittivities of the PET and PMMA are $3.2-j0.002$ and $2.25-j0.001$, respectively. The periodicity of the unit cell is $p = 12.9$ mm.

In order to simulate the periodical array of the proposed absorber, a finite element based solver with master and slave boundaries and the floquet ports is adopted. The absorptivity A can be calculated from the S parameters as $A = 1 - |S_{11}|^2 - |S_{21}|^2$. To maximize the absorptivity A , the reflection $|S_{11}|$ and the transmission $|S_{21}|$ are simultaneously minimized. In order to prevent the incident plane wave from penetrating through the absorber, the ITO film with the resistance of 6 Ω /sq acting as a ground is used. Fig. 2 shows the S parameters and the absorptivity of the

**FIGURE 1.** Geometry of the designed unit cell.**FIGURE 2.** Simulated S parameters and absorptivity of the proposed absorber.**FIGURE 3.** Simulated absorptivities of the proposed structure for different polarization angles.

proposed absorber when a plane wave is normally incident on it. It can be observed that the $|S_{11}|$ and $|S_{21}|$ of the designed absorber are less than -10 dB and -25 dB in a wide frequency band of 3.86~15.04 GHz, respectively. Therefore, the absorption over 90% can be obtained in the band covering 3.86~15.04 GHz with a fractional bandwidth of 118.3%. Note that the fractional bandwidth denotes the ratio of the absorption bandwidth over 90% to the central frequency.

Fig. 3 plots variation of the absorption with the polarization angle ϕ of the incident plane wave. As the polarization angle

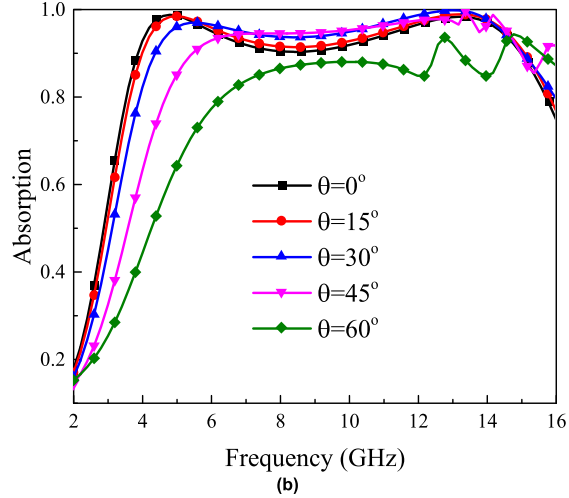
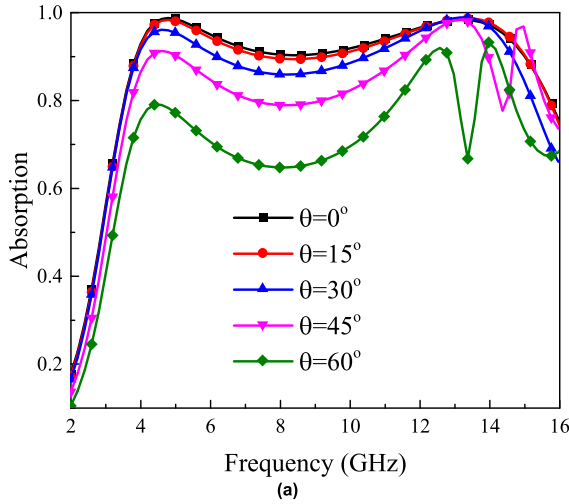


FIGURE 4. Simulated absorptivities of the structure for different incident angles under (a) TE polarization (b) TM polarization.

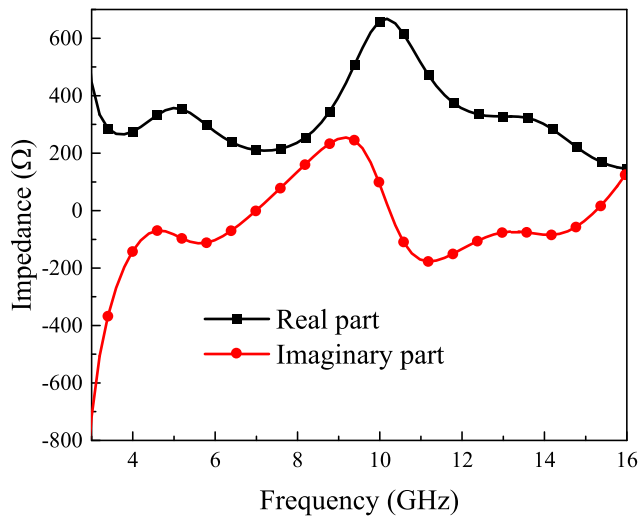


FIGURE 5. Equivalent impedance of the proposed transparent absorber.

φ varies from 0° to 45° , the absorptivity of the proposed transparent absorber keeps unchanged. The absorber is insensitive to the incident waves with different polarization angles, because the proposed absorber is of the symmetry.

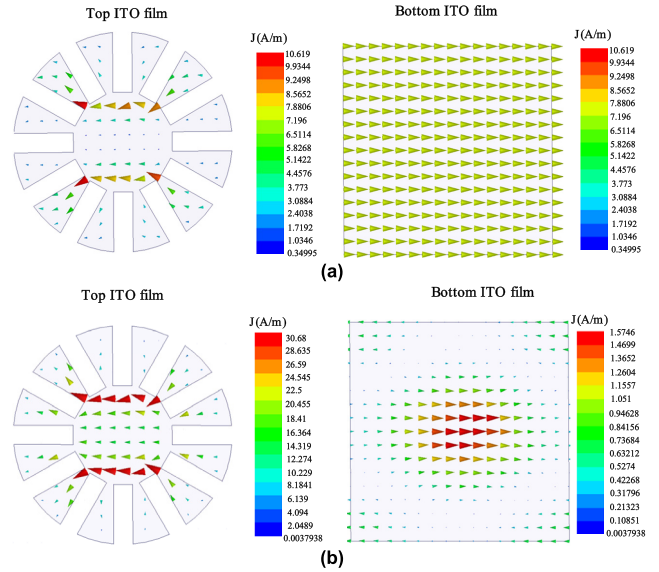


FIGURE 6. Surface current distributions of the transparent absorber at (a) 4.8 GHz (b) 13.6 GHz.

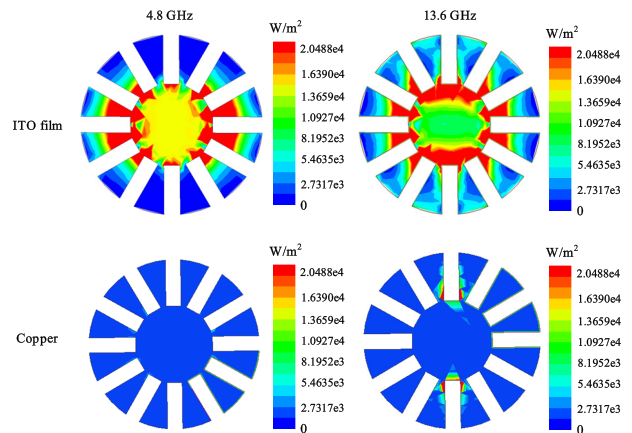


FIGURE 7. Surface loss density comparison between the copper based structure and the ITO film based structure at 4.8 GHz and 13.6 GHz.

The simulated absorptivities at oblique incidence under both TE and TM polarizations are shown in Fig. 4. It is found that the absorptions remain almost same with the increase of the incident angle θ of the plane wave from 0° to 30° under TE and TM polarizations in the frequency band of 3.86~15.04 GHz. When the incident angle θ continually increases from 30° to 45° , the absorptivity for the TE polarization gradually decreases. But the absorptivity larger than 80% is still obtained within entire frequency band. By comparison, the absorptivity for TM polarization is still over 90%, while the corresponding absorbing band gradually becomes narrow. This is because the mismatch impedance at large angle incidence degrades the absorption efficiency. With the further increase of the incidence angle θ from 45° to 60° , the absorptivity over 70% for TE polarization and the absorptivity over 80% for TM polarization, respectively, can be achieved in the frequency band. Hence the designed absorber has good incident angle stability.

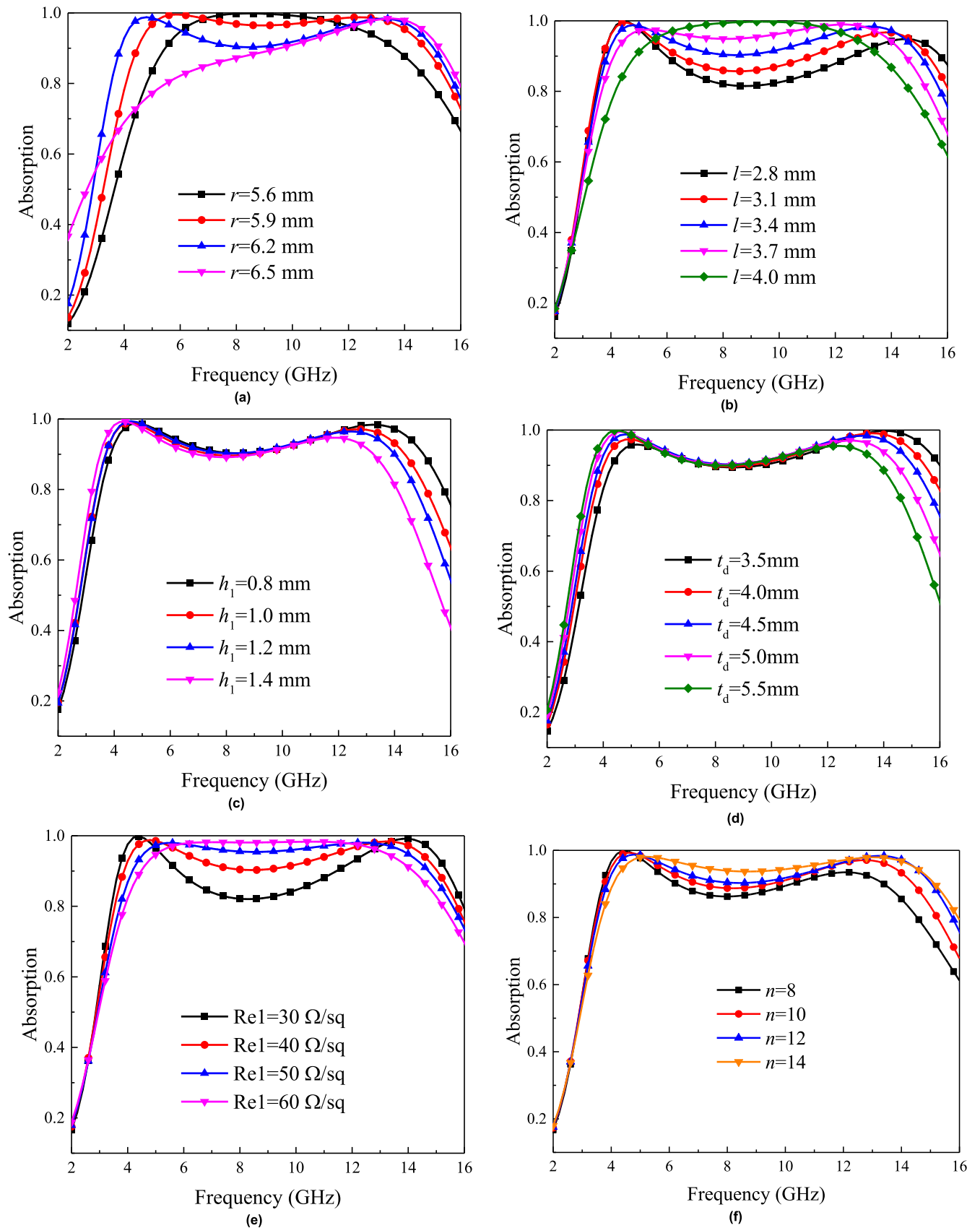


FIGURE 8. Variation of absorption with the geometric and material parameters. (a) r . (b) l . (c) h_1 . (d) t_d . (e) $Re1$. (f) n .

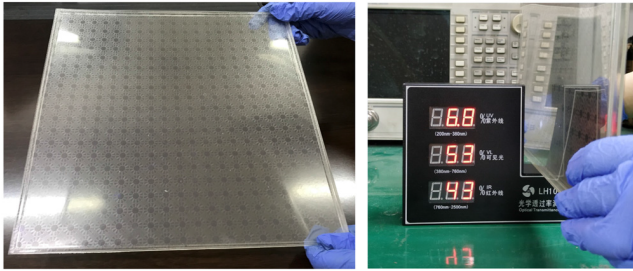


FIGURE 9. Transparent absorber prototype and its light transmittance.

B. ABSORBING MECHANISM ANALYSIS

In order to elaborate the absorbing mechanism of the proposed absorber, equivalent impedance, surface loss property, surface current distribution, and structure parameters of the absorber, respectively, are analyzed in this section.

Firstly, we investigate the equivalent impedance η of the proposed transparent absorber, as shown in Fig. 5. Note that the equivalent impedance is calculated as $\eta = \eta_0 \sqrt{[(1 + S_{11})^2 - S_{21}^2] / [(1 - S_{11})^2 - S_{21}^2]}$, in which η_0 is wave impedance in free space. It can be seen from Fig. 5 that in the band covering 3.86-15.04 GHz, the impedance of the absorber slowly fluctuates in the range of free-space wave impedance, meaning that the proposed absorber has good impedance matching with the free space. Hence the plane wave illuminated on the absorber enters into it with reflections as less as possible.

According to Fig. 2, there are two absorbing peaks at 4.8 GHz and 13.6 GHz, respectively. We plot the surface current distributions on the top and bottom ITO films at 4.8 GHz and 13.6 GHz, respectively, when a plane wave is normally incident on the absorber, as shown in Fig. 6. At 4.8 GHz, the surface currents on the top ITO film flow along the electric field, thus giving rise to the electric resonance. On the other hand, the surface currents on the top ITO film flow in an opposite direction to those on the bottom ITO film with the similar intensity, and therefore the magnetic resonant is generated. At 13.6 GHz, the resonant mode is only electric resonance generated by the current on the top ITO film. This is because the magnitudes of the surface currents on the bottom ITO film are far less than those on the top ITO film. Hence the perfect absorptivity at the high frequency band results from electric resonance while both electric and magnetic resonances lead to high absorption in low band.

In the following, dissipation of the electromagnetic wave in the transparent absorber is investigated. Fig. 7 shows the comparison of surface loss density between the proposed absorber and the reference structure. Here the reference structure is the same as the proposed absorber except that the ITO films are replaced by the coppers. It can be found that electromagnetic wave is hardly absorbed by the reference structure, which means that the absorption of the proposed transparent absorber mainly results from the ITO films.

Next, we investigate the absorption as functions of the geometric and material parameters, as shown in Fig. 8. As shown

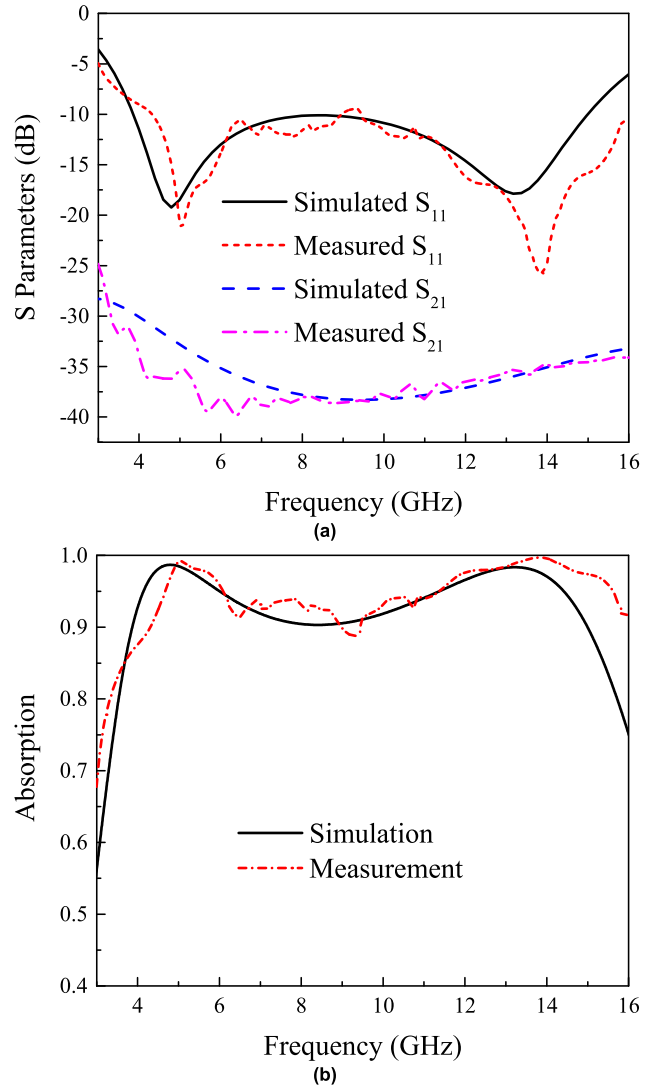


FIGURE 10. Comparison of the simulated and measured results under normal incidence. (a) S parameters. (b) Absorption.

in Fig. 8(a), when the radius r of the gear-shaped ITO film increases from 5.6 mm to 5.9 mm, the first resonant mode moves towards lower frequencies and meanwhile the second resonant mode shifts towards higher frequencies. With the increase of the radius r from 5.9 mm to 6.2 mm, the first resonant mode continuously moves towards lower frequencies with weaker resonant intensity, while the second resonant mode keeps unchanged. With $r = 6.5$ mm, the first resonant mode completely disappears. It can be seen from Fig. 8(b) that when the length l of the gear-shaped ITO film increases from 2.8 mm to 4.0 mm, the first resonant mode keeps unchanged at first and then shifts towards higher frequencies, and the second resonant mode always moves towards low frequencies. According to Fig. 8(c), the second resonant mode shifts towards high frequencies with the fixed first resonant mode as the thickness h_1 of the upper PMMA substrate decreases. As shown in Fig. 8(d), a similar case can be observed for the thickness of the air spacer t_d . It can

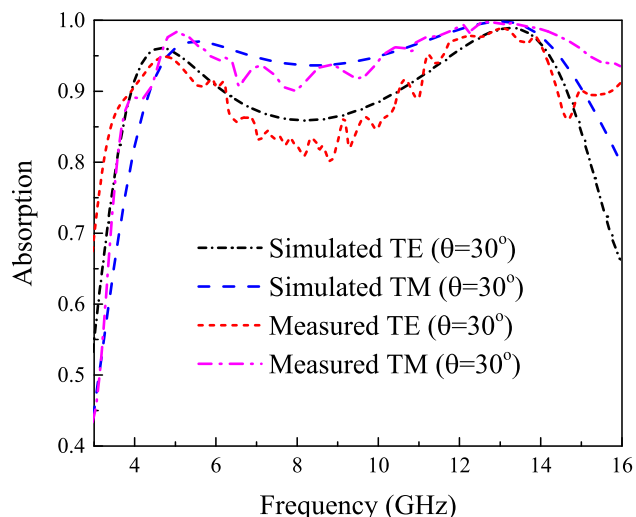


FIGURE 11. Comparison of the simulated and measured results under oblique incidence.

be observed from Fig. 8(e) that with the increase of the resistance of the upper ITO film, two resonant frequencies become increasingly close. When the resistance of the bottom ITO film Re_2 is less than $20 \Omega/\text{sq}$, the plane wave cannot penetrate through it and the resultant absorption performance keeps unchanged. As shown in Fig. 8(f), as the number of the gear teeth n increases, the second resonant mode continuously moves towards higher frequencies with a slightly shift of the first resonant mode towards higher frequencies. Therefore, in order to achieve the wide band characteristic, the optimized geometric and material parameters are chosen as follows: $r = 6.2 \text{ mm}$, $l = 3.4 \text{ mm}$, $h_1 = h_2 = 0.8 \text{ mm}$, $t_d = 4.5 \text{ mm}$, $Re_1 = 40 \Omega/\text{sq}$, $Re_2 = 6 \Omega/\text{sq}$, and $n = 12$.

III. EXPERIMENTAL RESULTS

In this section, performance of the proposed transparent absorber will be demonstrated by experiment. The absorber consisting of the 21×21 unit cells is fabricated and its whole size is $270.9 \text{ cm} \times 270.9 \text{ cm}$. A transparent acrylic glass square frame with 4.5 mm thickness is used as the air spacer between two ITO-PET-PMMA structures. The entire prototype is shown in Fig. 9. It can be observed that due to use of transparent materials, the light transmittance of 53% can be achieved.

The prototype was measured in an anechoic chamber. Here the space wave method [3] and time-domain measurement system are used for the measurements of both normal and oblique incidence cases. In experimental setup, a pair of horn antennas are connected to the vector network analyzer. In order to eliminate the influence of multiple reflections and diffractions of electromagnetic wave, the time-domain gate is reasonably chosen. The reflection and transmission coefficients of the sample are measured and normalized by those of a copper plate with the identical dimensions of the sample. The comparison of S parameters and corresponding absorption between the simulation and the measurement

TABLE 2. Absorption comparison between the proposed absorber and reported absorbers.

Transparent absorber	Centre frequency (GHz)	-10 dB bandwidth	Dielectric constant	Thickness (mm)
Ref. [16]	12.85	9.1 (70.8%)	2.25	3.85(0.247 λ_g)
Ref. [15]	10.36	8.6 (83.01%)	1	5(0.173 λ_g)
Ref. [20]	16.5	14 (84.84%)	3	5.5(0.524 λ_g)
Ref. [18]	18.4	20.6 (112%)	5.5	3.3(0.47 λ_g)
Proposed structure	9.45	11.2 (118.1%)	2.25	6.1(0.218 λ_g)

under normal and oblique incidences are shown in Figs. 10 and 11, respectively. A good agreement between the simulation and the measurement is observed to show the wide absorbing frequency band of $3.86 \sim 15.04 \text{ GHz}$ with a fractional bandwidth of 118.3%. According to simulation and measurement results, good absorption performance can be obtained for the incident angle of 30° under both TE and TM polarizations. The fluctuation of the measured results is due to fabricated tolerances including fabrication flatness, material errors and the use of the acrylic square frame.

Furthermore, Table 2 gives the absorbing performance comparison between the proposed transparent absorber with the reported transparent structures. It can be seen from Table 2 that the wider fractional absorption band of 118.1% can be achieved by the proposed transparent absorber with a relatively thin thickness of $0.218\lambda_g$, compared with the reported transparent absorbers.

IV. CONCLUSION

In this paper, a broadband microwave absorber with the optically transparent property has been designed. The absorber consists of two ITO-PET-PMMA structures with an air spacer. With the different surface resistances of two ITO films, the electromagnetic resonance and the electric resonance are generated at lower and higher frequencies, respectively. The proposed transparent absorber is of low profile, polarization insensitivity and angle stability. Measured results are given to exhibit the wide absorption band of $3.86 \sim 15.04 \text{ GHz}$ with a fractional bandwidth of 118.3%.

REFERENCES

- [1] E. F. Knott, J. F. Schaeffer, and M. T. Tuley, *Radar Cross Section*. Raleigh, NC, USA: SciTech, 2004.
- [2] K. J. Vinoy and R. M. Jha, *Radar Absorbing Materials: From Theory to Design and Characterization*. Norwell, MA, USA: Kluwer, 1996.
- [3] N. I. Landy, S. Sajuyigbe, J. J. Mock, D. R. Smith, and W. J. Padilla, "Perfect metamaterial absorber," *Phys. Rev. Lett.*, vol. 100, May 2008, Art. no. 207402.
- [4] W. W. Salisbury, "Absorbent body for electromagnetic waves," U.S. Patent 2599944 A, Jun. 10, 1952.
- [5] R. L. Fante and M. T. McCormack, "Reflection properties of the Salisbury screen," *IEEE Trans. Antennas Propag.*, vol. 36, no. 10, pp. 1443–1454, Oct. 1988.

- [6] Y. Shi, Y. C. Li, T. Hao, L. Li, and C.-H. Liang, "A design of ultra-broadband metamaterial absorber," *Waves Random Complex Media*, vol. 27, no. 2, pp. 381–391, Apr. 2017.
- [7] F. Ding, Y. Cui, X. Ge, Y. Jin, and S. He, "Ultra-broadband microwave metamaterial absorber," *Appl. Phys. Lett.*, vol. 100, no. 10, 2012, Art. no. 103506.
- [8] M. Li, S. Xiao, Y. Y. Bai, and B. Z. Wang, "An ultrathin and broadband radar absorber using resistive FSS," *IEEE Antennas Wireless Propag. Lett.*, vol. 11, pp. 748–751, 2012.
- [9] Y. Shi, J. Yang, H. Shen, Z. Meng, and T. Hao, "Design of broadband metamaterial-based ferromagnetic absorber," *Mater. Sci. Adv. Compos. Mater.*, vol. 2, no. 2, pp. 1–7, 2018.
- [10] S. Li, J. Gao, X. Cao, W. Li, Z. Zhang, and D. Zhang, "Wideband, thin, and polarization-insensitive perfect absorber based on the double octagonal rings metamaterials and lumped resistances," *J. Appl. Phys.*, vol. 116, no. 4, 2014, Art. no. 043710.
- [11] J. Sun, L. Liu, G. Dong, and J. Zhou, "An extremely broad band metamaterial absorber based on destructive interference," *Opt. Express*, vol. 19, no. 22, pp. 21155–21162, 2011.
- [12] B. Zhang and Z. Shen, "Wideband radar absorbing material combining high-impedance transmission line and circuit analogue screen," *Electron. Lett.*, vol. 44, no. 4, pp. 318–319, Feb. 2008.
- [13] Y. Zhang, Y. Shi, and C.-H. Liang, "Broadband tunable graphene-based metamaterial absorber," *Opt. Mater. Express*, vol. 6, no. 9, pp. 3036–3044, 2016.
- [14] S. Lai, Y. Wu, X. Zhu, W. Gu, and W. Wu, "An optically transparent ultrabroadband microwave absorber," *IEEE Photon. J.*, vol. 9, no. 6, Dec. 2017, Art. no. 5503310.
- [15] R. Deng, M. Li, B. Muneer, Q. Zhu, Z. Shi, L. Song, and T. Zhang, "Theoretical analysis and design of ultrathin broadband optically transparent microwave metamaterial absorbers," *Materials*, vol. 11, no. 1, p. 107, Jan. 2018.
- [16] K. Takizawa and O. Hashimoto, "Transparent wave absorber using resistive thin film at V-band frequency," *IEEE Trans. Microw. Theory Techn.*, vol. 47, no. 7, pp. 1137–1141, Jul. 1999.
- [17] B. Wu, H. M. Tuncer, M. Naem, B. Yang, M. T. Cole, W. I. Milne, and Y. Hao, "Experimental demonstration of a transparent graphene millimetre wave absorber with 28% fractional bandwidth at 140 GHz," *Sci. Rep.*, vol. 4, no. 2, 2014, Art. no. 4130.
- [18] D. Yi, X.-C. Wei, and Y.-L. Xu, "Transparent microwave absorber based on patterned graphene: Design, measurement, and enhancement," *IEEE Trans. Nanotechnol.*, vol. 16, no. 3, pp. 484–490, May 2017.
- [19] M. Haruta, K. Wadai, and O. Hashimoto, "Wideband wave absorber at X frequency band using transparent resistive film," *Microw. Opt. Technol. Lett.*, vol. 24, no. 4, pp. 223–226, 2000.
- [20] H. Shaokand, G. Singh, S. Ghoah, J. Ramkumar, S. A. Ramakrishna, and K. V. Srivastava, "An optically transparent broadband microwave absorber using interdigital capacitance," *IEEE Antennas Wireless Propag. Lett.*, vol. 18, no. 1, pp. 113–117, Jan. 2019.
- [21] H. Sheokand, S. Ghosh, G. Singh, M. Saikia, K. V. Srivastava, S. A. Ramakrishna, and J. Ramkumar, "Transparent broadband metamaterial absorber based on resistive films," *J. Appl. Phys.*, vol. 122, Aug. 2017, Art. no. 105105.
- [22] C. Zhang, Q. Cheng, J. Yang, J. Zhao, and T. J. Cui, "Broadband metamaterial for optical transparency and microwave absorption," *Appl. Phys. Lett.*, vol. 110, no. 14, 2017, Art. no. 143511.
- [23] I.-P. Hong and I.-G. Lee, "Transparent circuit analog electromagnetic absorber for window applications," in *Proc. 9th Eur. Conf. Antennas Propag. (EuCAP)*, Lisbon, Portugal, Apr. 2015, pp. 1–4.
- [24] S.-C. Tian, H. Xue, and L. Li, "An broadband transparent metamaterial absorber using an ITO resistive-film," in *Proc. 14th Int. Workshop Antenna Technol. (iWAT)*, Nanjing, China, Mar. 2018, pp. 1–3.
- [25] Z. Yin, Y. Lu, S. Gao, J. Yang, W. Lai, Z. Li, and G. Deng, "Optically transparent and single-band metamaterial absorber based on indium-tin-oxide," *Int. J. RF Microw. Comput. Aided Eng.*, vol. 29, no. 2, 2019, Art. no. e21536.
- [26] Y. Shen, J. Zhang, Y. Pang, J. Wang, H. Ma, and S. Qu, "Transparent broadband metamaterial absorber enhanced by water-substrate incorporation," *Opt. Express*, vol. 26, no. 12, pp. 15665–15674, 2018.
- [27] D. Hu, J. Cao, W. Li, C. Zhang, T. Wu, Q. Li, Z. Chen, Y. Wang, and J. Guan, "Optically transparent broadband microwave absorption metamaterial by standing-up closed-ring resonators," *Adv. Opt. Mater.*, vol. 5, no. 13, May 2017, Art. no. 1700109.
- [28] Y. Cheng, Y. Nie, X. Wang, and R. Gong, "Adjustable low frequency and broadband metamaterial absorber based on magnetic rubber plate and cross resonator," *J. Appl. Phys.*, vol. 115, no. 6, 2014, Art. no. 064902.
- [29] J. Yang and Z. Shen, "A thin and broadband absorber using double-square loops," *IEEE Antennas Wireless Propag. Lett.*, vol. 6, pp. 383–391, 2007.



LIN ZHANG received the B.E. degree in electronic information science and technology from Shanxi University, Shanxi, China, in 2014. She is currently pursuing the Ph.D. degree in electromagnetics and microwave technology with Xidian University, Xi'an, China. Her research interests include metamaterial, metasurface, cloak, and absorbing structure.



YAN SHI (M'07–SM'16) received the B.Eng. and Ph.D. degrees in electromagnetic fields and microwave technology from Xidian University, Xi'an, China, in 2001 and 2005, respectively.

He joined the School of Electronic Engineering, Xidian University, in 2005, where he was promoted to Full Professor, in 2011. From July 2007 to July 2008, he was a Senior Research Associate with the City University of Hong Kong, Hong Kong. From September 2009 to September 2010, he was a Visiting Postdoctoral Research Associate with the University of Illinois at Urbana–Champaign. From June 2017 to July 2017, he was a Visiting Professor with the State Key Laboratory of Millimeter Wave, City University of Hong Kong. He has authored or coauthored over 100 articles in referred journal, a book, and a chapter. His research interests include computational electromagnetics, metamaterial, antenna, and wireless power transfer.

Dr. Shi is a Senior Member of the Chinese Institute of Electronics (CIE). He received the Program for New Century Excellent Talents in University awarded by the Ministry of Education of China, in 2011, the New Scientific and Technological Star of Shaanxi Province awarded by the Education Department of Shaanxi Provincial Government, in 2013, the First Prize of Awards for Scientific Research Results of High Education of Shaanxi Province awarded by the Education Department of Shaanxi Provincial Government, in 2013, and the Second Prize of Awards of Science and Technology awarded by the Shaanxi Province Government, in 2015.



JIN XI YANG received the B.E. degree in electronic engineering from Xidian University, Xi'an, China, in 2017, respectively, where she is currently pursuing the master's degree in electromagnetics and microwave technology. Her research interests include machine learning, metasurface, and antenna array design.



XUAN ZHANG received the B.E. degree in electronic information science and technology from Xidian University, Xi'an, China, in 2018, respectively, where she is currently pursuing the master's degree in electromagnetics and microwave technology. Her research interests include antenna design and metasurface.



LONG LI (M'06–SM'11) was born in Anshun, Guizhou, China. He received the B.E. and Ph.D. degrees in electromagnetic fields and microwave technology from Xidian University, Xi'an, China, in 1998 and 2005, respectively.

In 2005, he joined the School of Electronic Engineering, Xidian University, where he was promoted to Associate Professor, in 2006. He was a Senior Research Associate with the Wireless Communications Research Center, City University of Hong Kong, in 2006. He received the Japan Society for Promotion of Science (JSPS) Postdoctoral Fellowship. He visited Tohoku University, Sendai, Japan, as a JSPS Fellow, from November 2006 to November 2008. He was a Senior Visiting Scholar with Pennsylvania State University, USA, from December 2013 to July 2014. He is currently a Professor with the School of Electronic Engineering, Xidian University. His research interests include metamaterials, computational electromagnetics, electromagnetic compatibility, novel antennas, and wireless power transfer technology. He is also a Senior Member of the Chinese Institute of Electronics (CIE). He received the Nomination Award of National Excellent Doctoral Dissertation of China, in 2007, the Best Paper Award at the International Symposium on Antennas and Propagation, in 2008, the Program for New Century Excellent Talents in University of the Ministry of Education of China, in 2010, the First Prize of Awards for Scientific Research Results offered by the Shaanxi Provincial Department of Education, China, in 2013, and the IEEE APS Raj Mittra Travel Grant Senior Researcher Award, in 2014.

...